Colloids and Surfaces A: Physicochem. Eng. Aspects 374 (2011) 108–114

Contents lists available at ScienceDirect

Colloids and Surfaces A: Physicochemical and Engineering Aspects

journal homepage: www.elsevier.com/locate/colsurfa

Copper, mercury and chromium adsorption on natural and crosslinked chitosan films: An XPS investigation of mechanism

Rodrigo S. Vieira [a], Mona Lisa M. Oliveira [b], Eric Guibal [c], Enrique Rodríguez-Castellón [b], Marisa M. Beppu [a,*]

[a] Departamento de Termofluidodinâmica, Faculdade de Engenharia Química, Universidade Estadual de Campinas, Caixa Postal 6066, Barão Geraldo, CEP 13081-970, Campinas, SP, Brazil
[b] Departamento de Química Inorgânica, Cristalografía y Mineralogía, Facultad de Ciencias, Unidad Asociada del Instituto de Catálisis y Petroleoquímica, CSIC, Universidad de Málaga, Campus de Teatinos, 29071 Málaga, Spain
[c] Ecole des Mines d'Alès, Laboratoire Génie de l'Environnement Industriel, 6 Avenue de Clavières, F-30319 Ales Cedex, France

ARTICLE INFO

Article history:
Received 24 May 2010
Received in revised form 8 November 2010
Accepted 10 November 2010
Available online 18 November 2010

Keywords:
Biopolymers
Heavy metals
Adsorption mechanism
XPS

ABSTRACT

Although biopolymers are focusing the attention of researchers as potential adsorbents for heavy metal removal, little information is given about the properties of the resulting complexes. This information would also bring a better understanding of the mechanisms involved in metal binding to the polymer. XPS (X-ray photo-electron spectroscopy) is a powerful technique to investigate how metal ions bind onto these matrices. In this study, copper, chromium and mercury ions were adsorbed on natural and crosslinked (glutaraldehyde and epichlorohydrin) chitosan matrices, which present diverse functional groups and may induce different adsorption mechanisms. X-ray photoelectron spectroscopy (XPS) revealed that these metals bind to glutaraldehyde-crosslinked chitosan, differently from the other two kinds of matrices. Hence, amino group availability and the formation of new structures such as imino bonds are key factors. Copper(II) stabilization was found to be poor in glutaraldehyde-crosslinked chitosan. Conversely, Hg(II) ions present higher adsorption capacity in this kind of matrix. Chromium(VI) was reduced in all three matrices. In this case, chromium(VI) is probably not well stabilized by the functional groups of these polymers and may also undergo the action of their reducing groups.

1. Introduction

In the last years, environment contamination by heavy metals has gained much attention due to the significant impact on public health. Chromium, mercury and copper are used in several industrial applications and are recognized as agents that present toxic effect to humans and other living beings.

Chitin is the second most abundant natural polymer in the world after cellulose. Upon deacetylation yields chitosan, a linear polysaccharide based on glucosamine units, has been described as a biopolymer suitable to be used for removal of heavy metal ions from wastewater [1–7] since its chemical groups can act as chelation sites. Most of the studies on heavy metal adsorption have been dedicated to the determination of the overall uptake performance; however, there is still limited information available on identifying the adsorption mechanisms.

Sophisticated analytical techniques, like XPS [8–11], Mössbauer spectrometry [12], XANES and EXAFS [13–15], can be used to identify surface groups that are primarily responsible for binding metallic species and also for the state of adsorbed metals. X-ray photoelectron spectroscopy (XPS) technique has been used for characterizing the structure of metal compounds and their interactions with membranes and films constituted by polymers [16–18], as well their interactions with catalysts [19,20], algal biomass [21], yeast [22], and synthetic sorbents [23–24]. Dambies et al. [8] used XPS to characterize the functional groups involved in the adsorption mechanisms of Cu(II), Cr(VI) and Mo(VI) on chitosan (flakes or beads conditioning) and to analyze the possible reduction mechanism of these species after adsorption. The present study used XPS technique to identify the sorption sites involved in the accumulation of adsorbed species and determines the oxidation state of metal ions after adsorption process. Natural and crosslinked chitosan films (using glutaraldehyde and epichlorohydrin as crosslinkers) were used [25], in order to determine the optimum experimental conditions for sorption when using each of these adsorbents.

Fig. 1 depicts possible structures formed by crosslinking using glutaraldehyde and epichlorohydrin, respectively [5,26]. Crosslinking reactions are usually carried out in order to prevent chitosan dissolution in acidic solutions or to improve metal

* Corresponding author. Tel.: +55 19 3788 3893; fax: +55 19 3788 3922.
E-mail address: beppu@feq.unicamp.br (M.M. Beppu).

0927-7757 © 2010 Elsevier B.V. Open access under the Elsevier OA license.
doi:10.1016/j.colsurfa.2010.11.022

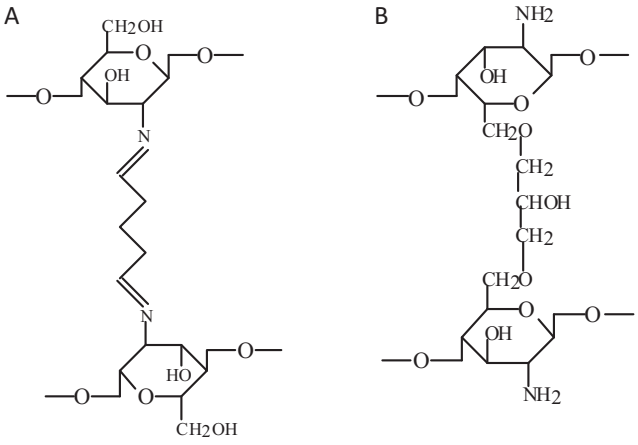

Fig. 1. Possible structures formed by crosslinking using glutaraldehyde and epichlorohydrin (A), (B), respectively.

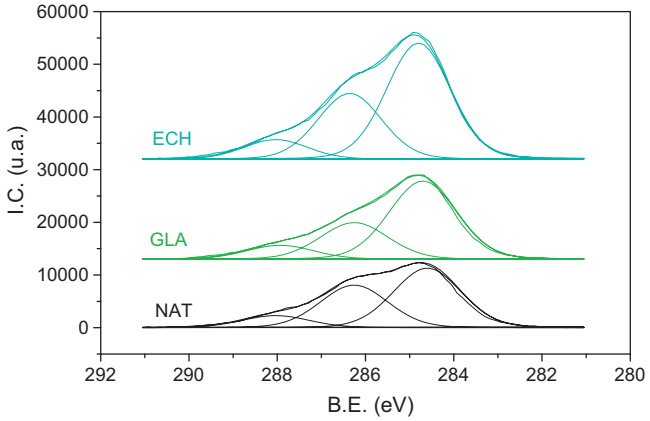

Fig. 2. C 1*s* XPS of natural (NAT) and crosslinked chitosan (GLA and ECH) films.

adsorption properties, i.e., to increase capacity or to enhance selectivity.

2. Experimental methods

2.1. Materials

Chitosan (commercial grade) was purchased from Sigma (USA): the deacetylation degree was 85% and the molecular weight was 9.9×10^5 g/g mol. All other chemicals were of analytical grade. The aqueous solutions were prepared using deionized water (Milli-Q ultrapure water).

2.2. Preparation and chemical modification of chitosan films

In order to prepare the films, chitosan was dissolved in aqueous acetic acid 3% (v/v) solution, producing a final viscous solution with 2.5% (w/w) biopolymer concentration. This solution was then spread on Petri dishes that were kept at 60 °C until constant weight was reached. Afterwards, membranes were immersed in a solution of NaOH (1 mol L^{-1}) for 24 h in order to neutralize the amino groups. The films were exhaustively washed with distilled water until reaching neutral pH and stored in water at the temperature of 4 °C [27].

Pristine chitosan films were heterogeneously crosslinked by contacting with a 0.75% (w/w) aqueous glutaraldehyde solution (3.0 g of wet chitosan film in 50 mL of glutaraldehyde solution) without stirring, at room temperature for 2 h, followed by rinsing with deionized water to remove unreacted glutaraldehyde residues. The crosslinking with epichlorohydrin was performed by immersing wet raw chitosan films (3.0 g) in 50 mL of a 0.01 mol L^{-1} epichlorohydrin solution (prepared in 0.067 mol L^{-1} NaOH solution) at 40 °C, under continuous agitation for 2 h [5–7]. Finally, the films were rinsed with deionized water to remove unreacted epichlorohydrin.

2.3. Adsorption on chitosan films

Metal adsorption was performed by soaking chitosan films in metal solutions (500 mg L^{-1} of Cu (as sulfate), Hg (as chloride) and Cr (as potassium dichromate)) in batch experiments. The pH of metal solution was adjusted using NaOH solution (0.1 mol L^{-1}) and was kept at 4.5, 5.0 and 4.0, for Cu, Hg and Cr, respectively.

It is important to note that precipitation did not occur at the concentration and pH used. After adsorption, an extensive rinsing step is always necessary to remove the solution that is absorbed in the matrices and that may contain metal ions that would produce artifacts in results.

After adsorption, the films were air dried at room temperature in order to perform XPS analysis.

2.4. XPS analysis

The XPS measurements were carried out with a spectrometer (model Physical Electronics 5700), using an Mg-Kα source (1253.6 eV) (model 04-548 Dual Anode X-rays Source). The X-ray source was run at a power of 300 W (10 keV and 30 mA). The pressure inside the vacuum chamber was 5×10^{-8} torr. A hemispherical analyzer was employed (10-360 Precision Energy Analyzer) with a multi-channel detector (16 channels, which uses a chevron pair of multi-channel plates with 16 discretes anodes and 16 channels of amplification, discrimination and counting electronics). The lens system (Omni Focus IV Lens) was used to scan the spectrum and to define the size of the analysis area. All spectra were obtained using a 720 μm diameter analysis area. Chitosan samples were mounted on a stainless steel sample holder and stored overnight under vacuum in the preparation unit before being transferred to the analysis chamber of the spectrometer. The specimens were analyzed at an angle of 45°, to the surface plane. The X-ray source was located at 54° position relatively to the analyzer axis. A short acquisition time of 10 min was used to examine C 1*s*, Cu 2*p* and Cu LMM XPS regions in order to avoid, as much as possible, photoreduction of Cu(II) species. The spectra were recorded by using the Physical Electronics PC-Access ESCA-V6.0F software. Binding energies (BE) were referred to the C 1*s* line of adventitious carbon at 284.8 eV and determined with the resolution of ±0.1 eV. These spectra were fitted assuming Gaussian–Lorentzian distribution for each peak, with a linear background in order to determine the binding energy of the various element core levels.

3. Results and discussion

3.1. Adsorbent characterization

XPS analysis was initially conducted for adsorbents prior to adsorption in order to characterize the available functional groups. The studied material could be characterized by recording the photoemission bands C 1*s*, N 1*s* and O 1*s*. Fig. 2 shows the core level C 1*s* spectrum for natural and crosslinked chitosan films. The C 1*s* signal were decomposed in three peaks and the binding energy (BE) of the three peaks and their assignment are included in Table 1 (that summarizes the identification of signals observed in natural and crosslinked chitosan XPS spectra, and their atomic fractions). There is C 1*s* from C–C, C–N, C=N, O–C–O and C=O. The bound C=O

Table 1
Assignments of main spectral bands based on their binding energies (BE) and atomic concentration (AC) for natural and crosslinked chitosan films.

Element	Natural chitosan		GLA-chitosan		ECH-chitosan		Assignments
	BE (eV)	AC (%)	BE (eV)	AC (%)	BE (eV)	AC (%)	
C 1*s*	284.6	36.2	284.7	44.0	284.8	41.3	C–C or adventitious carbon
C 1*s*	286.2	25.9	286.3	20.7	286.4	24.0	C–N, C=N, C–O or C–O–C
C1*s*	288.0	7.3	287.9	7.8	288.0	7.1	C=O or O–C–O
Total C		69.4		72.5		73.4	
O 1*s*	532.4	22.4	532.6	20.8	532.6	21.2	–C–O or O–H or bound water
N 1*s*	399.4	6.2	399.5	4.0	399.4	4.9	N
					401.0	0.4	NH_3^+
Total N		6.2		4.0		5.3	
Si 2*p*	103.3	2.0	102.5	2.7	102.0	1.1	SiO_2 contamination

can be attributed to acetyl groups from chitosan backbone. In our system, a ΔBE of 0.5 eV is significant.

Results indicate that the atomic concentration (%) of C–C groups increases with the chemical modification and surface changes. This increase in atomic concentration of aliphatic carbon (C–C) can be interpreted as a result of the addition of alkyl groups induced by crosslinking reactions. The crosslinking with glutaraldehyde reduces the intensity of the C 1*s* peak at 286.3 eV, indicating the formation of new bonds, such as imino bonds (C=N). The N 1*s* signal is not affected by the crosslinking treatment since nitrogen from amino and imino groups exhibit N 1*s* photoemissions at similar BE's [28], confirming that the structure is homogeneous in terms of nitrogen sites. The O 1*s* bands are slightly affected by the chemical modification, as expected by introduction of crosslinker groups.

Table 2 shows the theoretical and experimental C/N and C/O ratios for natural and crosslinked chitosan. The theoretical C/N and C/O for crosslinked chitosan was calculated assuming two chitosan monomers for one glutaraldehyde or epichlorohydrin molecule. The atomic concentration of oxygen was calculated by diminishing the oxygen amount present in SiO_2 (that was detected and that probably comes as chitosan contaminant). A little relative error was observed, due to the precision limit of the experimental technique, but the numbers were in very good agreement with the expected results. Variations can possibly be caused by side-reactions and polymerization of crosslinkers that can occur as known in the literature [29].

3.2. Copper adsorption on natural and crosslinked chitosan films

The complexation properties of chitosan has been reported for various metal ions [1–7], however, the precise mechanism and the molecular geometry of complexation by different functional groups of chitosan, needs to be more studied and discussed. Different models have been proposed to the mechanism of coordination during the formation of complexes. It is generally accepted that copper binds to nitrogen with the formation of a single complex, called "pendant model", or another possibility is that the metallic ion is bound to several nitrogen atoms from the same or different chains [30].

Table 3 summarizes the identification of the bands observed on the XPS spectra for natural and crosslinked chitosan films after copper adsorption. Fig. 3 shows the core level C 1*s* spectrum for natural and crosslinked chitosan films after metal adsorption.

Table 2
Theoretical and experimental C/N and C/O ratio of natural and crosslinked chitosan.

	C/N		C/O	
	Theoretical	Experimental	Theoretical	Experimental
Natural chitosan	6.0	6.4	2.0	2.1
GLA-chitosan	8.5	8.9	2.8	2.2
ECH-chitosan	7.5	7.4	2.1	2.2

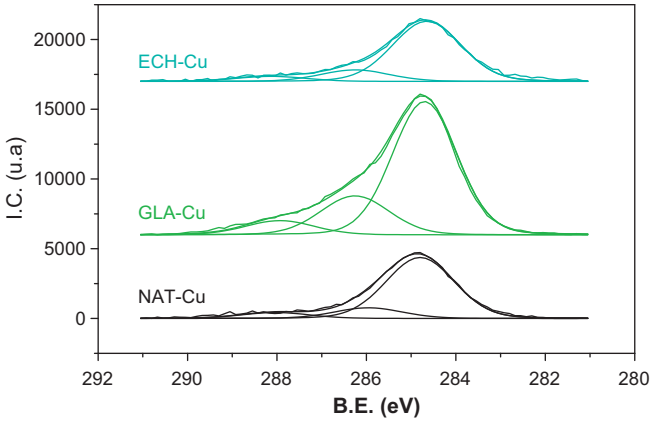

Fig. 3. C 1*s* XPS of natural (NAT) and crosslinked chitosan (GLA and ECH) films after copper adsorption.

A decrease in the atomic concentration for C 1*s* was observed for natural and epiclorohydrin-crosslinked chitosan, compared to the material before Cu adsorption. For glutaraldehyde-crosslinked chitosan, the same concentration was observed before and after adsorption. Cu 2*p* core level signals exhibit a high intensity for natural and epiclorohydrin-crosslinked chitosan than that for glutaraldehyde-crosslinked chitosan (see Fig. 4).

Fig. 4 shows a representative XPS spectrum of Cu 2*p* core regions acquired from chitosan films and its appropriate curve-fit. The spectrum noise is attributed to the short acquisition time that had to

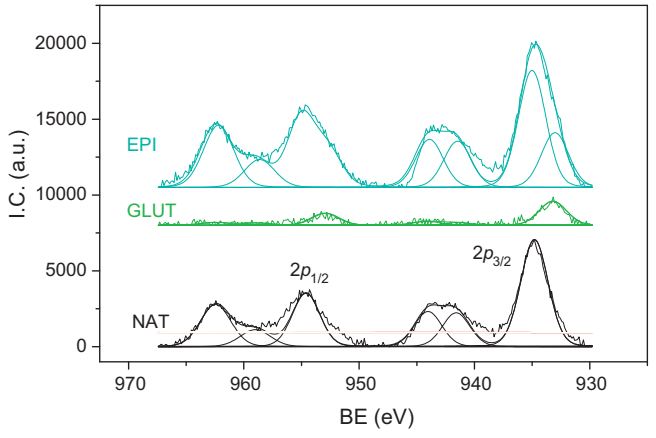

Fig. 4. Cu 2*p* XPS of natural (NAT) and crosslinked chitosan (GLA and ECH) films after cooper adsorption.

Table 3
Assignments of main spectral bands based on their binding energies (BE) and atomic concentration (AC) for natural and crosslinked chitosan films after copper adsorption.

Element	Natural chitosan		GLA-chitosan		ECH-chitosan		Assignments
	BE (eV)	AC (%)	BE (eV)	AC (%)	BE (eV)	AC (%)	
C 1*s*	284.8	24.9	284.7	51.5	284.6	20.8	C–C or adventitious carbon
C 1*s*	286.0	4.4	286.3	16.0	286.3	4.0	C–N, C=N, C–O or C–O–C
C1*s*	288.0	2.5	287.9	5.8	288.1	1.7	C=O or O–C–O
Total C		31.8		73.3		26.5	
O 1s	531.8	43.9	532.4	19.1	531.6	48.1	–C–O or O–H or bound water
N 1s	397.4	5.1	399.8	2.7	397.4	2.4	N
Si 2*p*	103.3	2.0	102.2	3.7		2.0	SiO_2 contamination
S 2*p*			168.2	0.7	168.6	6.0	
Cu $2p_{3/2}$	934.8	13.8	933.2	0.5	933.4 935.0	15.0	
CuLMM	336.9		338.6		338.9		

be used in order to avoid the photo-reduction of Cu(II) ions, by the action of X-rays [31,32]. A large symmetric peak with a maximum at 934.8 eV can be seen in the Cu $2p_{3/2}$ core region for natural chitosan, at 933.2 eV for glutaraldehyde-crosslinked chitosan, and a large asymmetric signal that can be decomposed in two contributions at 933.4 eV (32%) and 935.0 eV (68%) for epiclorohydrin-crosslinked chitosan (Table 3). The peak-fit of the Cu $2p_{3/2}$ core level reveals two binding energy states for epiclorohydrin-crosslinked chitosan, which can be assigned to CuO [33] and cupric ions residing in octahedral sites and strongly interacting with crosslinked chitosan [34], respectively. Surface Cu(II) ions are in an octahedral environment, in contrast with the copper spinel structure, where copper occupies predominantly the tetrahedral sites [35]. The existence of a Cu $2p_{3/2}$ photoemission at 934.8 eV for natural chitosan is also assigned to the cupric ions strongly interacting with crosslinked chitosan, that is, ion-exchanged Cu(II). In the XPS spectrum for glutaraldehyde-crosslinked chitosan, only a symmetric peak of Cu $2p_{3/2}$, at 933.2 eV is observed and its assignation is difficult due to the low intensity of the signal, but also to the low values of the shake up satellite/main peak ratio, probably due to a reduction to Cu(I). Shake-up lines at ca. 944 and 962 eV for the Cu $2p_{3/2}$ and $2p_{1/2}$ core levels, respectively, are the evidence of an open $3d^9$ shell of Cu(II) [36]. The binding energy states resulting from the peak-fit of XPS Cu $2p_{3/2}$ core level and the relative intensities of the shake-up lines to the main core level of the Cu $2p_{3/2}$ level are given in Table 4. Since the XPS signal of Cu(I) does not present shake-up features, the presence of Cu(II) and Cu(I) can be estimated from the Cu $2p_{3/2}$ shake-up satellite/main peak ratio. Marked reduction of the Cu(II) states for glutaraldehyde crosslinked chitosan is indicated by a decrease in the satellite to main peak ratio of the Cu $2p_{3/2}$ level. It is also important to establish whether reduction occurs to Cu(I) or Cu(0). Since the XPS spectra for these two oxidation states are indistinguishable, the Auger spectra of the Cu LMM transition have been used to determine the modified Auger parameter, α_0, calculated from the following equation:

$$\alpha'_0 = KE_{CuLMM} - KE_{Cu2p3/2} + 1253.6$$

Table 4
Electronic parameters of copper for natural and crosslinked chitosan.

Parameter	Sample		
	Natural chitosan	GLA-chitosan	ECH-chitosan
Peak-fit of the Cu $2p_{3/2}$ core level			
BE state 1(eV)	934.8 (100%)	933.2 (100%)	933.4 (68%)
BE state 2 (eV)			935.0 (32%)
Satellite to main peak ratio	0.46	0.28	0.58
Cu modified Auger Parameter	1851.5	1848.0	1850.7

where KE_{CuLMM} is the kinetic energy of the CuLMM Auger electron, $KE_{Cu2p3/2}$ is the kinetic energy of the Cu $2p_{3/2}$ photoelectron and 1253.6 is the energy of the Mg Kα X-ray excitation source in eV. The α'_0 values obtained for the natural and crosslinked chitosan films are summarized in Table 4. The Cu Auger parameters of the most appropriate reference compounds are as follows: 1851.6 eV, CuO; 1849.3 eV, Cu_2O; and 1851.3 eV, Cu metal [37]. Direct comparison with these references is difficult to be done, since anomalous α'_0 values are observed for Cu(II) in the present study. The bigger decrease in the Auger parameter was observed for glutaraldehyde-crosslinked chitosan, which indicates the appearance of Cu(I) species rather than Cu(0).

In fact, the presence of these reduced specimens could be either attributed to the interaction with chitosan, known as good antioxidant agents for metals [38,39] or could also be a result from the specific experimental conditions that have to be applied in XPS analysis, of high and endured vacuum. The reduction mechanism can be interpreted as the result of two mechanisms: (i) chitosan, as well as its monomers and polysaccharides contains reducing ends. These reducing ends are oxidized in acidic media causing the reduction of some metal ions; (ii) the reduction step is enhanced when the solution is exposed to light (solar or UV light).

However, independently of the possibility of an experimental artifact, the differences among chitosan matrices can still be explored, as all samples underwent the same preparation and analyses condition. The fact that the reduction only occurred better in glutaraldehyde-crosslinked matrices, indicate that the binding of oxidized forms of copper ion are probably less stable in this environment, where less amino groups are available and more imino and crosslinking structures are present [40]. The multi-valent model of copper atoms binding to more than one functional group would find less anchoring sites in glutaraldehyde-crosslinked matrices. As a consequence, copper would be more loosely attached to the functional groups of this kind of matrix. A weaker pendant model would be more suitable to represent the structure and, in this case, would deal an increased tendency to also present reduced copper as possible output.

3.3. Mercury adsorption on natural and crosslinked chitosan films

Fig. 5 presents the core level C 1*s* spectrum for natural and crosslinked chitosan films after mercury adsorption. Table 5 reports the binding energies and the main assignments after mercury adsorption. A decrease in the atomic concentration for C 1*s* was observed for all three adsorbents, in comparison to the material before adsorption, indicating the good capacity of matrices to adsorb and incorporate Hg(II) ions, mainly in glutaraldehyde-crosslinked chitosan. This result is in accordance

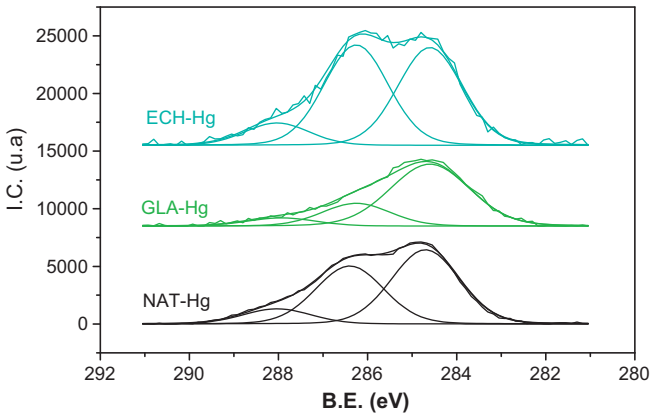

Fig. 5. C 1*s* XPS of natural (NAT) and crosslinked chitosan (GLA and ECH) films after mercury adsorption.

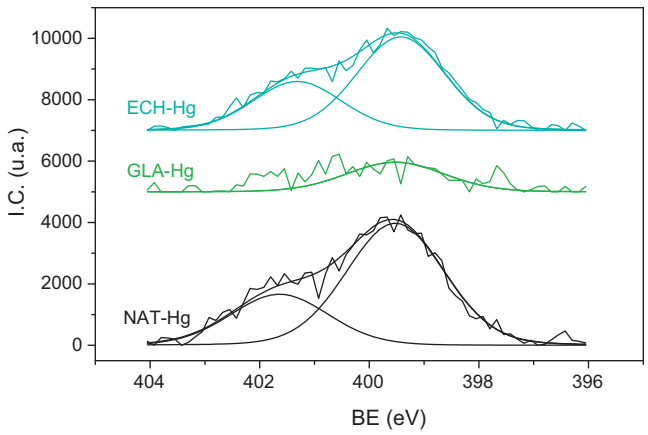

Fig. 6. N 1*s* for natural (NAT) and crosslinked chitosan (GLA and ECH) films after mercury adsorption.

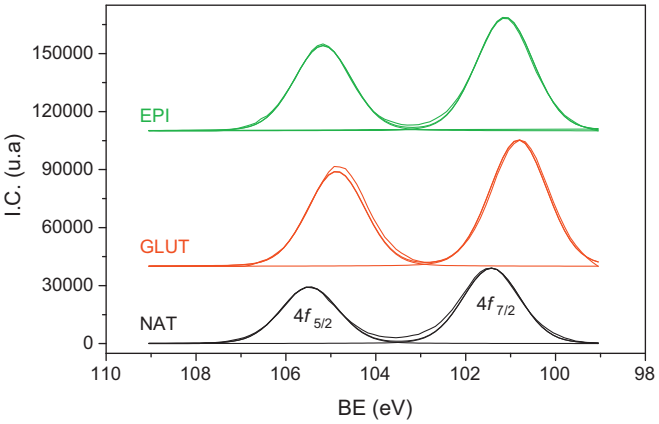

Fig. 7. Hg 4*f* for natural (NAT) and crosslinked chitosan (GLA and ECH) films after mercury adsorption.

with the adsorption results obtained from static experiments, which indicate that glutaraldehyde-crosslinked chitosan presented the highest adsorption capacity for Hg(II) ions [5,6]. A reduction in the intensity of the C 1*s* (286.3 eV) for glutaraldehyde-crosslinked chitosan (Table 5) indicates that mercury adsorption can take place on the structure resulting from primary amino and aldehyde terminal (imino bound), not discarding the possibility of interaction with hydroxyl and non reacted amino groups that are also present in natural and epichlorohydrin-crosslinked chitosan matrices.

The other differences observed among XPS spectra are identified on nitrogen band with the appearance of a new band 401.3–401.6 eV for natural and epichlorohydrin-crosslinked chitosan. Fig. 6 presents N 1*s* spectrum after Hg adsorption. It is possible to observe that some of the nitrogen sites are free (constant BE) whilst others are submitted to a charge transfer from amino sites to mercury. This shift can also be attributed to the protonation of nitrogen sites. In the case of glutaraldehyde-crosslinked chitosan, the N 1*s* signal is very weak; this is probably due to the high amount of Hg taken up (see Table 5). This heavy metal ion is totally recovering the amino groups avoiding its detection at the surface.

Fig. 7 shows the Hg 4*f* core level signals for the studied samples after Hg adsorption. The vacuum pressure in the analysis chamber decreased during all spectral acquisitions, indicating that mercury is reduced and released into the analysis chamber, which can correspond to unreacted mercury. However, a phase change induced on samples by the X-ray irradiation and the ultra high vacuum can also be considered as the mean cause. For both natural and crosslinked chitosan, mercury adsorption is followed by the appearance of a doublet (Hg $4f_{5/2}$ and $4f_{7/2}$) with symmetric peaks. These peaks were decomposed into only one component. A decrease in the BE of Hg $4f_{7/2}$ can be observed for glutaraldehyde-crosslinked chitosan. The BEs of Hg $4f_{7/2}$ of the most appropriate reference compounds are as follows: 101.4 eV ($HgCl_2$); 108.0 eV (HgO) and 99.8 (Hg metal). For natural and epichlorohydrin-crosslinked chitosan, it is possible to assume that the adsorbed mercury species are in $HgCl_2$ form and for glutaraldehyde-crosslinked chitosan case, either $HgCl_2$ and HgO would be possible. Again, the glutaraldehyde-crosslinked material shows a different behavior and mechanism when compared to the other two versions of biopolymers that would present more free amino groups: glutaraldehyde-crosslinked chitosan has imino

Table 5
Assignments of main spectral bands based on their binding energies (BE) and atomic concentration (AC) for natural and crosslinked films after mercury adsorption.

Element	natural chitosan		GLA-chitosan		ECH-chitosan		Assignments
	BE (eV)	AC (%)	BE (eV)	AC (%)	BE (eV)	AC (%)	
C 1*s*	284.7	29.5	284.6	37.0	284.6	25.0	C–C or adventitious carbon
C 1*s*	286.4	23.0	286.3	11.7	286.3	25.7	C–N, C=N, C–O or C–O–C
C 1*s*	288.0	6.0	287.9	4.2	288.0	5.7	C=O or O–C–O
Total C		58.5		52.9		56.4	
O 1*s*	532.7	23.0	532.2	14.2	532.4	22.8	–C–O or O–H or bound water
N 1*s*	399.7		399.5		399.4		N
	401.6				401.3		NH_3^+
Total N		4.1		2.4		5.2	
Si 2*p*	153.3	2.5				1.3	SiO_2 contamination
Hg $4f_{7/2}$	101.4	3.4	100.8	15.9	101.1	6.8	

Table 6
Assignments of main spectral bands based on their binding energies (BE) and atomic concentration (AC) for natural and crosslinked chitosan films after chromium adsorption.

Element	Natural chitosan		GLA-chitosan		ECH-chitosan		Assignments
	BE (eV)	AC (%)	BE (eV)	AC (%)	BE (eV)	AC (%)	
C 1*s*	284.7	40.3	284.8	60.1	284.7	41.6	C– or adventitious carbon
C 1*s*	286.3	18.9	286.4	12.6	286.3	19.3	C–, C=N, C–O or C–O–C
C 1*s*	288.0	7.1	288.0	5.6	288.0	7.7	C=O or O–C–O
Total C		66.3		78.3		68.6	
O 1*s*	532.6	23.9	532.5	16.5	532.3	25.7	–C–O or O–H or bound water
N 1*s*	399.9	4.1	399.5	2.1	399.7	2.8	N
N 1s					401.0	0.7	NH_3^+
Total N		4.1		2.1		3.5	
Si 2*p*		3.4	102.5	2.1	1.8	2.5	
Cr $2p_{3/2}$	577.0	1.8	577.0	1.1	576.9	2.3	Cr(III)

groups, a more soft basic ligand than amino or hydroxyl groups, and this ligand should interact with a very soft acid such as Hg(II). This fact can explain the high adsorption capacity of glutaraldehyde-crosslinked chitosan for Hg(II) in comparison with the other studied biopolymers.

3.4. Chromium adsorption on natural and crosslinked chitosan films

Fig. 8 depicts the typical XPS spectra for natural and crosslinked chitosan films after chromium adsorption. Table 6 summarizes the identification of the bands observed in Fig. 8. Comparing these results with the ones observed before adsorption (Table 1), a decrease in the atomic concentration of C 1*s* can be noticed in natural and epichlorohydrin crosslinked chitosan, and an increase is seen in glutaraldehyde-crosslinked chitosan. This increase occurs mainly at BE 284.7 eV and is related to carbon contamination. At BE 286.4 eV, a decrease was observed related to C–N or C=N bonds, indicating that chromium adsorption can take place either on imino or on hydroxyls and non reacted amino groups.

This study was performed with an initial Cr(VI) solution (500 mg/L – pH 6.0), in order to evaluate both adsorption and reduction mechanism. Fig. 9 shows a representative XPS spectrum of Cr 2*p* core regions acquired from chitosan films and its appropriated curve-fit. The appearance of peaks for Cr $2p_{3/2}$ at 577.0 and 576.9 eV can be observed. The BEs for Cr $2p_{3/2}$ are assigned at 577.4 eV ($CrCl_3$), 577.3 eV ($Cr(OH)_3$) and 576.2 eV (Cr_2O_3) to Cr(III), whilst Cr(VI) are characterized by higher binding energies such as at 578.1 eV (CrO_3) and 579.9 eV ($K_2Cr_2O_7$). In this way, it is possible to affirm that there is only Cr(III), and all Cr(VI) was reduced.

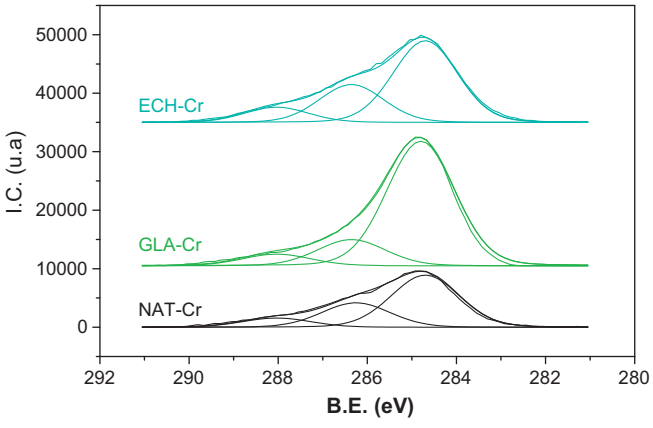

Fig. 8. C 1*s* for natural (NAT) and crosslinked chitosan (GLA and ECH) films after chromium adsorption.

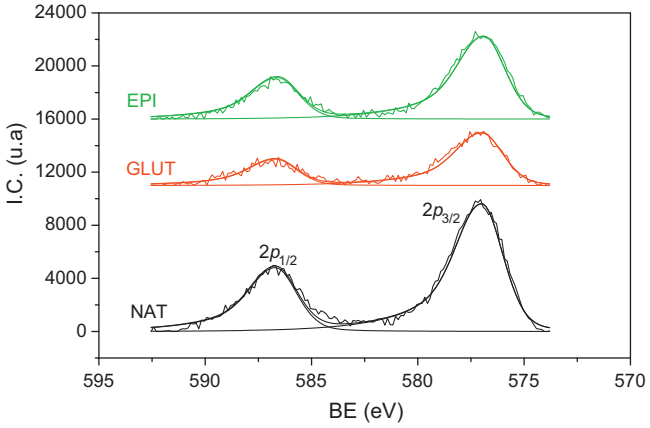

Fig. 9. Cr 2*p* for natural (NAT) and crosslinked chitosan (GLA and ECH) films after chromium adsorption.

Again, the same comment about the experimental conditions, mentioned for copper, would be applied here. However, this result is in accordance with others reported in the literature. Dambies et al. [8] observed that all Cr(VI) is reduced for Cr(III) on crosslinked chitosan bead. They have found only 60% of the chromium in its reduced form, on natural chitosan, and this extent could have been enhanced by XPS experimental vacuum conditions. Chromium(VI) species would bind to natural and crosslinked chitosan differently as copper ions do: chromium ions would be reduced more easily in natural and crosslinked chitosan matrices than copper ions as expected by their normal redox potential [41]. The latter would be reduced easily only in glutaraldehyde-crosslinked matrices. Probably, the more multivalent (VI and III) nature of chromium ion would indicate that only a multi-group interaction would stabilize this kind of ion, with not only amino groups but other groups being necessary to accomplish this stabilization.

4. Conclusions

XPS analysis confirmed that chitosan crosslinking with glutaraldehyde and epichlorohydrin occurs preferentially on amino and hydroxyl groups leading to final structures with different functional groups.

Copper reduction was detected after adsorption on glutaraldehyde-crosslinked chitosan, indicating that natural and epichlorohydrin-crosslinked chitosan would expose functional groups that might stabilize better the adsorbed copper in a divalent form. Conversely, chromium binds to chitosan being reduced in each of the matrices tested. In this case, multi-valent nature of chromium is probably hardly stabilized by the functional groups of polymeric matrices.

Finally, mercury ions would bind well onto natural and crosslinked chitosan, but again, with different mechanism in glutaraldehyde-crosslinked chitosan, which would involve more chemical groups to metal ions justifying the higher adsorption capacity found for this specific type of matrix.

Acknowledgements

The authors thank FAPESP for financial support and CNPq for the scholarship of R. Vieira.

References

[1] K.H. Chu, Removal of copper from aqueous solution by chitosan in prawn shell: adsorption equilibrium and kinetics, J. Hazard. Mater. B90 (2002) 77–95.
[2] E. Guibal, Interactions of metal ions with chitosan-based sorbents: a review, Sep. Purif. Technol. 38 (2004) 43–74.
[3] D. Merrifield, W.G. Davids, J.D. MacRae, A. Amirbahman, Uptake of mercury by thiol-grafted chitosan gel beads, Water Res. 38 (2004) 3132–3138.
[4] D. Zhou, L. Zhang, G. Shenglian, Mechanisms of lead biosorption on cellulose/chitin beads, Water Res. 39 (2005) 3755–3762.
[5] R.S. Vieira, M.M. Beppu, Interaction of natural and crosslinked chitosan membranes with Hg(II) ions, Colloids Surf. A: Physicochem. Eng. Aspects 279 (2006) 196–207.
[6] R.S. Vieira, M.M. Beppu, Dynamic and static adsorption and desorption of Hg(II) ions on chitosan membranes and spheres, Water Res. 40 (2006) 1726–1734.
[7] P. Baroni, R.S. Vieira, E. Meneghetti, M.G.C. da Silva, M.M. Beppu, Evaluation of batch adsorption of chromium ions on natural and crosslinked chitosan membranes, J. Hazard. Mater. 152 (2008) 1155–1163.
[8] L. Dambies, C. Guimon, S. Yiacoumi, E. Guibal, Characterization of metal ion interactions with chitosan by X-ray photoelectron spectroscopy, Colloids Surf. A: Physicochem. Eng. Aspects 177 (2001) 203–214.
[9] A.L. da Róz, F.L. Leite, L.V. Pereiro, P.A.P. Nascente, V. Zucolotto, O.N. Oliveira Jr., A.J.F. Carvalho, Adsorption of chitosan on spin-coated cellulose films, Carbohydr. Polym. 80 (2010) 65–70.
[10] F. Peirano, T. Vincent, F. Quignard, M. Robitze, E. Guibal, Palladium supported on chitosan hollow fiber for nitrotoluene hydrogenation, J. Membr. Sci. 329 (2009) 30–45.
[11] L. Fras, L.S. Johansson, P. Stenius, J. Laine, K. Stana-Kleinschek, V. Ribitsch, Analysis of the oxidation of cellulose fibers by titration and XPS, Colloids Surf. A: Physicochem. Eng. Aspects 260 (2005) 101–108.
[12] S.C. Bhatia, N.A. Ravi, A magnetic study of an Fe−chitosan complex and its relevance to other biomolecules, Biomacromolecules 1 (2000) 413–417.
[13] J.L. Gardea-Torresdey, J.R. Peralta-Videa, G. de la Rosa, J.G. Parsons, Phytoremediation of heavy metals and study of the metal coordination by X-ray absorption spectroscopy, Coord. Chem. Rev. 249 (2005) 1797–1810.
[14] J.L. Gardea-Torresdey, K.J. Tiemann, V. Armendariz, L. Bess-Oberto, R.R. Chianelli, J. Rios, J.G. Parsons, G. Gamez, Characterization of Cr(VI) binding and reduction to Cr(III) by the agricultural byproducts of *Avena monida* (Oat) biomass, J. Hazard. Mater. B80 (2000) 175–188.
[15] J.L. Gardea-Torresdey, K. Dokkena, K.J. Tiemann, J.G. Parsons, J. Ramos, N.E. Pingitor, G. Gamez, Infrared and X-ray absorption spectroscopic studies on the mechanism of chromium(III) binding to alfalfa biomass, Microchem. J. 71 (2002) 157–166.
[16] M.Z.A. Yahya, A.K. Arof, Conductivity and X-ray photoelectron studies on lithium acetate doped chitosan films, Carbohydr. Polym. 55 (2004) 95–100.
[17] A.K. Arof, N.M. Morni, M.A. Yarmo, Evidence of lithium-nitrogen interaction in chitosan-based films from X-ray photoelectron spectroscopy, Mater. Sci. Eng. B55 (1998) 130–133.
[18] S. Chen, G. Wu, H. Zengb, Preparation of high antimicrobial activity thiourea chitosan–Ag+ complex, Carbohydr. Polym. 60 (2005) 33–38.
[19] P.A.P. Nascente, Materials characterization by X-ray photoelectron spectroscopy, J. Mol. Catal. A: Chem. 228 (2005) 145–150.
[20] V.I. Bukhtiyarov, V.V. Kaichev, I.P. Prosvirin, X-ray photoelectron spectroscopy as a tool for in-situ study of the mechanisms of heterogeneous catalytic reactions, Top. Catal. 32 (2005) 3–15.
[21] J.P. Chen, L. Yang, Study of a heavy metal biosorption onto raw and chemically modified Sargassum sp. via spectroscopic and modeling analysis, Langmuir 22 (2006) 8906–8914.
[22] R. Ashkenazy, L. Gottlieb, S. Yannai, Characterization of acetone-washed yeast biomass functional groups involved in lead biosorption, Biotechnol. Bioeng. 55 (1997) 1–10.
[23] J.P. Rawat, A. Ahmad, A. Agrawal, Equilibrium studies for the sorption of Cu2+ on lanthanum diethanolamine – a chelating material, Colloids Surf. 46 (1990) 239–253.
[24] R. Moreno-Tost, E. Rodríguez-Castellón, A. Jiméenez-López, Cobalt-iridium impregnated zirconium-doped mesoporous silica as catalysts for the selective catalytic reduction of NO with ammonia, J. Mol. Catal. A: Chem. 248 (2006) 126–134.
[25] M.M. Beppu, R.S. Vieira, C.G. Aimoli, C.C. Santana, J. Membr. Sci. 301 (2007) 126–134.
[26] C. Chang, B. Duan, L. Zhang, Fabrication and characterization of novel macroporous cellulose-alginate hydrogels, Polymer 50 (2009) 5467–5473.
[27] M.M. Beppu, C.C. Santana, PAA influence on chitosan membrane calcification, Mater. Sci. Eng. C23 (2003) 651–658.
[28] J.F. Moulder, W.F. Stickle, P.E. Sobol, K.D. Bomben, Standard Spectra for Identification and Interpretation of XPS Data, Perkin Elmer, Eden Prairie, MN, 1992.
[29] A. Simionescu, D. Simionescu, R. Deac, Lysine-enhanced glutaraldehyde cross-linking of collagenous biomaterials, J. Biomed. Mater. Res. 25 (1991) 1495–1505.
[30] A. Domard, pH and cd measurements on a fully deacetylated chitosan–application to Cu(II)–polymer interactions, Int. J. Biol. Macromol. 9 (1987) 98–104.
[31] S. Poulston, P.M. Parlett, P. Stone, M. Bowker, Surface oxidation and reduction of CuO and Cu_2O studied using XPS and XAES, Surf. Interface Anal. 24 (1996) 811–820.
[32] E. Moretti, M. Lenarda, L. Storaro, A. Talon, T. Montanari, G. Busca, E. Rodríguez-Castellón, A. Jiménez-López, M. Turco, G. Bagnasco, R. Frattini, One-step synthesis of a structurally organized mesoporous $CuO–CeO_2–Al_2O_3$ system for the preferential CO oxidation, Appl. Catal. A: Gen. 335 (2008) 46–55.
[33] G. Ertl, R. Hierl, H. Knozinger, N. Thiele, H.P. Urbach, XPS study of copper aluminate catalysts, Appl. Surf. Sci. 5 (1980) 49–64.
[34] P.A. Berger, J.F. Roth, Copper oxide supported on alumina. 2. Electron spin resonance studies of highly dispersed phases, J. Phys. Chem. 71 (1967) 4307–4315.
[35] R.M. Friedman, J.J. Freeman, W. Lytle, Characterization of $Cu–Al_2O_3$ catalysts, J. Catal. 55 (1978) 10–28.
[36] M. Brandhorst, J. Zajac, D.J. Jonesa, J. Rozière, W. Womes, A. Jimenez-Lopez, E. Rodriguez-Castellón, Cobalt-, copper- and iron-containing monolithic aluminosilicate-supported preparations for selective catalytic reduction of NO with NH_3 at low temperatures, Appl. Catal. B: Environ. 55 (2005) 267–276.
[37] J.P. Espinos, J. Morales, A. Barranco, A. Caballero, J.P. Holgado, A.R. Gonzalez-Elipe, Interface effects for Cu, CuO, and Cu_2O deposited on SiO_2 and ZrO_2 XPS determination of the valence state of copper in Cu/SiO_2 and Cu/ZrO_2 catalysts, J. Phys. Chem. B 106 (2002) 6921–6929.
[38] B. Geng, Z. Jin, T. Li, Z. Qi, Preparation of chitosan-stabilized Fe-0 nanoparticles for removal of hexavalent chromium in water, Sci. Total Environ. 407 (2009) 4994–5000.
[39] S.J. Wu, T.H. Liou, F.L. Mi, Synthesis of zero-valent copper–chitosan nanocomposites and their application for treatment of hexavalent chromium, Bioresour. Technol. 100 (2009) 4348–4353.
[40] E. Guibal, J. Roussy, P. Le Cloirec, Photochemical reaction of uranium with glucosamine, acetylglucosamine and related polymers: chitin and chitosan, Water S.A. 22 (1996) 19–26.
[41] K.E Abu-Saba, A.R. Flegal, D.L. Sedlak, Reduction of hexavalent chromium by copper in the presence of superoxide, Mar. Chem. 69 (2000) 33–41.